Atmospheric
Chemistry
and Physics

Effects of NO$_2$ and C$_3$H$_6$ on the heterogeneous oxidation of SO$_2$ on TiO$_2$ in the presence or absence of UV–Vis irradiation

Biwu Chu[1,2,3], **Yali Wang**[1,3,4], **Weiwei Yang**[1,3,5], **Jinzhu Ma**[1,2,3], **Qingxin Ma**[1,2,3], **Peng Zhang**[1], **Yongchun Liu**[1,6], and **Hong He**[1,2,3]

[1]State Key Joint Laboratory of Environment Simulation and Pollution Control, Research Center for Eco-Environmental Sciences, Chinese Academy of Sciences, Beijing 100085, China
[2]Center for Excellence in Regional Atmospheric Environment, Institute of Urban Environment, Chinese Academy of Sciences, Xiamen 361021, China
[3]University of Chinese Academy of Sciences, Beijing 100049, China
[4]Chinese Research Academy of Environmental Sciences, Beijing 100012, China
[5]Key Laboratory of Pesticide and Chemical Biology of Ministry of Education, Institute of Environmental and Applied Chemistry, College of Chemistry, Central China Normal University, Wuhan 430079, China
[6]Aerosol and Haze Laboratory, Beijing Advanced Innovation Center for Soft Matter Science and Engineering, Beijing University of Chemical Technology, Beijing 100029, China

Correspondence: Qingxin Ma (qxma@rcees.ac.cn)

Abstract. The heterogeneous reactions of SO$_2$ in the presence of NO$_2$ and C$_3$H$_6$ on TiO$_2$ were investigated with the aid of in situ diffuse reflectance infrared fourier transform spectroscopy (DRIFTS) under dark conditions or with UV–Vis irradiation. Sulfate formation with or without the coexistence of NO$_2$ and/or C$_3$H$_6$ was analyzed with ion chromatography (IC). Under dark conditions, SO$_2$ reacting alone resulted in sulfite formation on TiO$_2$, while the presence of parts per billion (ppb) levels of NO$_2$ promoted the oxidation of SO$_2$ to sulfate. The presence of C$_3$H$_6$ had little effect on sulfate formation in the heterogeneous reaction of SO$_2$ but suppressed sulfate formation in the heterogeneous reaction of SO$_2$ and NO$_2$. UV–Vis irradiation could significantly enhance the heterogeneous oxidation of SO$_2$ on TiO$_2$, leading to copious generation of sulfate, while the coexistence of NO$_2$ and/or C$_3$H$_6$ significantly suppressed sulfate formation in experiments with UV–Vis lights. Step-by-step exposure experiments indicated that C$_3$H$_6$ mainly competes for reactive oxygen species (ROS), while NO$_2$ competes with SO$_2$ for both surface active sites and ROS. Meanwhile, the coexistence of NO$_2$ with C$_3$H$_6$ further resulted in less sulfate formation compared to introducing either one of them separately to the SO$_2$–TiO$_2$ reaction system. The results of

this study highlighted the complex heterogeneous reaction processes that take place due to the ubiquitous interactions between organic and inorganic species and the need to consider the influence of coexisting volatile organic compounds (VOCs) and other inorganic gases in the heterogeneous oxidation kinetics of SO$_2$.

1 Introduction

Atmospheric aerosol pollution has attracted widespread attention in recent years because of its adverse effects on human health, visibility, and climate (Thalman et al., 2017; Davidson et al., 2005; Pöschl, 2005). In many developing countries, such as China and India, high concentrations of SO$_2$, NO$_x$, and volatile organic compounds (VOCs) coexist in the atmosphere (Zou et al., 2015; Liu et al., 2013; Yang et al., 2009) and result in "complex atmospheric pollution" (Yang et al., 2011) and heavy haze events. Sulfate was found to play important roles in the occurrence of these haze events (Zhang et al., 2011; Z. R. Liu et al., 2017) due to both its high mass concentration in fine particles (PM$_{2.5}$) and its strong hygroscopicity. Rapid formation of sulfate was frequently ob-

served in haze episodes in China, in which heterogeneous reactions played important roles (He et al., 2014; Zhang et al., 2006; Ma et al., 2018). However, the mechanism of the heterogeneous reaction process as well as its contribution to sulfate formation in complex atmospheric pollution remains uncertain (Yang et al., 2018; Ma et al., 2018; Wang et al., 2018; Yu and Jang, 2018). These uncertainties are considered to be the main reason for the inaccuracy of sulfate simulation in air quality models (Wang et al., 2014b; Zheng et al., 2015; Yu and Jang, 2018).

About 1000 to 3000 Tg of mineral aerosols are emitted into the atmosphere every year (Dentener et al., 1996; Shen et al., 2013; Jaoui et al., 2008) and provide abundant surface area for the heterogeneous oxidation of SO_2. The heterogeneous uptake of SO_2 can form bisulfite (HSO_3^-) or sulfite (SO_3^{2-}) on γ-Al_2O_3 and sulfate (SO_4^{2-}) on MgO (Goodman et al., 2001b). Similarly, SO_2 can be converted into sulfite, bisulfite, or sulfate on mineral dust such as metal oxides (Zhang et al., 2006), calcite, and Chinese loess (Usher et al., 2002). The heterogeneous reaction of SO_2 on mineral dust can be promoted by gaseous oxidants. For example, SO_2 could be oxidized into sulfate by O_3 on the surface of $CaCO_3$ particles (Li et al., 2006; Zhang et al., 2018). Similar results were obtained when introducing H_2O_2 into the heterogeneous oxidation system (Capaldo et al., 1999; Jayne et al., 1990). NO_2 can also promote the heterogeneous oxidation of SO_2. In our previous studies, it was found that SO_2 was oxidized to sulfate on γ-Al_2O_3 in the presence of NO_2 and O_2, while it was only converted to sulfite in the absence of them (Ma et al., 2008). Therefore, NO_2 was proposed to act as a catalyst in the oxidation of SO_2 by O_2, in which the intermediates observed in the spectra, i.e., nitrogen tetroxide (N_2O_4), might play an important role (Ma et al., 2008). This synergistic effect between SO_2 and NO_2 was further observed on many other mineral oxides such as CaO, α-Fe_2O_3, ZnO, MgO, α-Al_2O_3, and TiO_2 (Liu et al., 2012; Ma et al., 2017; Zhao et al., 2018; Yu et al., 2018). These effects were confirmed in smog chamber studies and field observations of heavy haze in China, and they were proposed to be an important reason for the rapid growth of sulfate in haze events (He et al., 2014; Ma et al., 2018; Wang et al., 2014a; Chu et al., 2016). Heterogeneous oxidation of SO_2 may also be affected by the coexistence of organic compounds. Pre-adsorption of acetaldehyde (CH_3CHO) was found to suppress the heterogeneous reaction of large amounts of SO_2 on the surface of α-Fe_2O_3 (Zhao et al., 2015), while HCHO was proposed to react with SO_3^{2-} and generate hydroxymethanesulfonate (HMS) in the northern China winter haze period (Moch et al., 2018; Song et al., 2019). Wu et al. (2013) found that the synergistic effects between formic acid (HCOOH) and SO_2 in the heterogeneous reaction on hematite provide a new source of sulfate.

UV illumination can affect both the properties of particles and heterogeneous reactions on them (Nanayakkara et al.,

2012; Cwiertny et al., 2008; George et al., 2015). The photooxidation of SO_2 in the presence of mineral dust may represent an important pathway for generating sulfate aerosols (Park et al., 2017; Yu and Jang, 2018). TiO_2, an n-type semiconductor material, has been widely used for studying heterogeneous photochemical reactions (Chen et al., 2012). TiO_2 can be excited by UV light ($\lambda < 387$ nm), resulting in electrons and holes that can react with O_2 and H_2O and produce $\cdot O_2^-$ and $\cdot OH$, respectively. These reactive oxygen species (ROS), primarily $\cdot O_2^-$ and $\cdot OH$, can participate in the heterogeneous oxidation of SO_2 on TiO_2 (Chen et al., 2012). Shang et al. (2010) studied the heterogeneous reaction of SO_2 on TiO_2 particles using in situ diffuse reflectance infrared fourier transform spectroscopy (DRIFTS) and observed that SO_2 was oxidized to sulfate on TiO_2 with UV illumination while remaining as sulfite under dark conditions. Our recent study showed that O_2 and H_2O have contrary roles in the photooxidation of SO_2 on TiO_2, where surface water exhibits a competition effect in the reaction of SO_2 due to the occupation of surface OH (Ma et al., 2019). Besides H_2O, the coexistence of organics may also suppress the formation of sulfate due to competition with SO_2 for reactive oxygen species. For example, Du et al. (2000) studied the photocatalytic reaction of SO_2 in the presence of heptane (C_7H_{16}) and found that the formation of sulfate was suppressed.

Despite these studies involving the heterogeneous oxidation of SO_2 under various conditions, the effects of coexisting pollutants on the heterogeneous oxidation of SO_2 under both dark and illuminated conditions need further investigation. Meanwhile, the interactions between organic and inorganic species in these heterogeneous processes at low concentrations are not fully understood. In this study, we focus on the effects of coexisting NO_2 and propene (C_3H_6) on the heterogeneous oxidation of SO_2 on TiO_2 under both dark and illuminated conditions with in situ DRIFTS. In order to better study the effects of NO_2 and C_3H_6 on the heterogeneous oxidation in a relatively complex oxidation system (with coexistence of multiple gases, in both dark and illuminated conditions), we chose TiO_2 due to the fact that it is a semiconductor material and a well-known photocatalyst. TiO_2 has been widely reported to be present in airborne particulate matter (PM) (Chen et al., 2012). Although TiO_2 represents only a relatively small portion of the mass of PM and is less abundant than CaO, Fe_2O_3, or MgO, the TiO_2 particles are expected to provide important surfaces for heterogeneous photocatalysis of atmospheric gases due to their high photocatalytic activity, especially with the growing application of TiO_2 in human activities (Chen et al., 2012). Propene is selected as a representative VOC since it is the most abundant alkene compound in the atmosphere, and it coexists with NO_x in vehicle exhaust emissions (Wang et al., 2016a). Propene is widely used as an accelerator in photochemical reactions in some smog chamber studies (Jang and Kamens, 2001; Song et al., 2007). The relatively simple ox-

idation products and well understood oxidation mechanism of propene are also helpful in explaining our experimental results. Propene is selected also due to the high vapor pressure of its oxidation products, which normally do not generate condensed organic aerosol (Odum et al., 1996). However, we must point out that the heterogeneous reactivity depends greatly on the properties of the mineral oxides, such as acid–base nature or redox properties (Tang et al., 2016; Yang et al., 2016, 2019), while different VOCs may also have quite different heterogeneous and photochemical reactivity. Investigating these processes on different mineral dust and authentic dust particles with different types of VOCs is needed in future studies. Rather than UV lights, a xenon light is used in this study to better simulate the solar ultraviolet radiation on the earth's surface. Generally, our study could be helpful for gaining a better understanding of the heterogeneous formation of sulfate under complex air pollution conditions, in which abundant SO_2, NO_x, VOCs, and mineral dust coexist in the atmosphere.

2 Experimental section

2.1 Materials

TiO_2 (Degussa P_{25}) used in this study is a typical commercially available material, which contains 75 % anatase and 25 % rutile. It has been widely used in laboratory studies due to its good photocatalytic properties. The surface area of the material in this study was $50.50 \, m^2 \, g^{-1}$, measured by an ASAP2010 BET apparatus with multipoint Brunauer–Emmett–Teller (BET) analysis. The average particle diameter was about 20 nm, determined by transmission electron microscopy (H-7500, Hitachi Inc.). For gases, N_2 (99.999 % purity, Beijing Huayuan) and O_2 (99.999 % purity, Beijing Huayuan) were introduced as synthetic air (80 % N_2 and 20 % O_2) in this study, while SO_2 (5.9 ppm in N_2, Beijing Huayuan), NO_2 (3.9 ppm in N_2, Beijing Huayuan), and C_3H_6 (5.9 ppm in N_2, Beijing Huayuan) were used as reactant gases.

2.2 Experimental methods

2.2.1 In situ DRIFTS

In situ diffuse reflectance infrared fourier transform spectroscopy (DRIFTS) spectra were recorded on a Nicolet Nexus 670 Fourier transform infrared spectroscope (FTIR) equipped with a mercury cadmium telluride (MCT) detector, scanning from 4000 to 650 cm^{-1} at a resolution of $4 \, cm^{-1}$ for 100 scans. Before each experiment, the oxide sample was finely ground and placed into a ceramic crucible in the in situ chamber. Then the sample was pretreated at 503 K and atmospheric pressure for 120 min to remove adsorbed species in $100 \, mL \, min^{-1}$ synthetic air. All the spectra are presented in the Kubelka–Munk (K-M) scale to improve the linear-

ity of the dependence of signal intensity upon concentration (Armaroli et al., 2004). The UV–Vis irradiation was acquired with 500 W xenon light (CHF-XM35, Beijing Changtuo) and was introduced into the DRIFTS reaction cell via a UV optical fiber. The intensity of UV–Vis irradiation was measured as $478 \, \mu W \, cm^{-2}$ by a UV meter (Photoelectric Instrument Factory of Beijing Normal University). The wavelengths of the UV–Vis irradiation were measured to be in the range of 300–800 nm by a fiber-optic spectrometer (BLUE-Wave-UVNb, Stellar Net Inc., USA), as shown in Fig. S1 in the Supplement. The spectrum of the UV–Vis irradiation is comparable to the spectrum of solar irradiation on the earth surface, and therefore we think the UV–Vis irradiation used in this study may represent the conditions in the real atmosphere.

To investigate heterogeneous sulfate formation in complex atmospheric pollution, in situ DRIFTS was used to analyze the products on particle surfaces in the reactions under different conditions. Two series of in situ DRIFTS experiments were carried out in this study. For the heterogeneous reaction of SO_2 under different gas conditions, the TiO_2 sample was initially flushed with the synthetic air at a total flow rate of $100 \, mL \, min^{-1}$ for 2 h. The temperature was 303 K and the relative humidity was less than 1 % in all experiments. Then the background spectra were recorded when they showed little change with time. After that, gas reactants, such as 200 ppb SO_2, 200 ppb NO_2, and 200 ppb C_3H_6, were introduced to the gas flow and then passed through the reaction chamber for 12 h. These experiments were carried out under both dark and with UV–Vis irradiation conditions. The other series of experiments were step-by-step exposure experiments for further investigation of the effects of NO_2 and C_3H_6 on the heterogeneous oxidation of SO_2 with UV–Vis irradiation. The concentrations of reactants in the step-by-step exposure experiments were changed from 200 ppb to 200 ppm to strengthen the signals of the products. These step-by-step exposure experiments all included three steps, namely first exposing the particles to NO_2, C_3H_6, or both for 2 h; flushing with air for 1 h; and finally exposing them to SO_2 for 2 h.

2.2.2 IC

Sulfate products on the powders after the in situ DRIFTS study were also measured quantitatively using ion chromatography (IC). The powders were firstly weighed and placed in 8 mL transparent glass jars. After adding 5 mL of ultrapure water (specific resistance $\geq 18.2 \, M\Omega \, cm^{-1}$) containing about 1 % formaldehyde (50 μL) to inhibit the oxidation of sulfite to sulfate, the samples were then extracted by sonication at 303 K for 120 min. After a standing time of 120 min, the obtained supernatant was passed through a 0.22 μm PTFE membrane filter and was then analyzed using a Wayee IC-6200 ion chromatograph equipped

with a Thermo AS14 analytical column. An eluent of 3.5 mM Na$_2$CO$_3$ was used at a flow rate of 0.8 mL min^{-1}.

3 Results

3.1 Heterogeneous reaction of SO$_2$ under different conditions

3.1.1 Heterogeneous reaction of SO$_2$ on TiO$_2$

DRIFTS spectra for heterogeneous reaction of 200 ppb SO$_2$ on TiO$_2$ under dark conditions or with UV–Vis irradiation are shown in Fig. 1, while the vibrational frequencies of chemisorbed species formed on the surface of TiO$_2$ are listed in Table 1. In the dark experiment, the reaction products on the surface of TiO$_2$ were mainly sulfite. As shown in Fig. 1a, the positive bands observed at 1098, 1078, and 1052 cm^{-1} can be assigned to monodentate sulfite (Hug, 1997; Peak et al., 1999). Negative peaks at 3691 and 3630 cm^{-1} were attributed to hydroxyl on TiO$_2$ (Primet et al., 1971; Tsyganenko and Filimonov, 1973; Ferretto and Glisenti, 2003). These negative peaks were observed in all the reaction systems in this study, as shown in Fig. 1, which is consistent with previous studies (Nanayakkara et al., 2012; Ma et al., 2019). The loss of surface hydroxyl groups from the surface upon adsorption of SO$_2$ implies that surface OH groups were involved in the reaction of SO$_2$ on TiO$_2$ under both dark and UV–Vis irradiation conditions.

With UV–Vis light illumination, SO$_2$ was oxidized on TiO$_2$ and resulted in abundant sulfate species, as shown in Fig. 1b. The main bands in the 1400–1100 cm^{-1} region became more apparent with increasing exposure time. The spectra in this region were assigned to sulfate in different coordination modes, including aggregation at 1344 cm^{-1}, bidentate at 1290 cm^{-1}, and bridging sulfate at 1177 and 1141 cm^{-1} (Hug, 1997; Peak et al., 1999; Fu et al., 2007). With UV–Vis illumination, TiO$_2$ can be excited by UV light ($\lambda < 387$ nm), and then the photogenerated electrons and holes can react with H$_2$O and O$_2$ to produce additional ROS (primarily ·O$_2^-$ and ·OH), which oxidize more SO$_2$ to sulfate on TiO$_2$ than that produced under dark conditions (Shang et al., 2010; Chen et al., 2012). The sharp band at 1626 cm^{-1} and the broad bands with maxima at 3316 and 3190 cm^{-1} in Fig. 1b can be assigned to the bending vibration and stretching modes of molecularly adsorbed water. Surface water can be formed in the heterogeneous reaction of SO$_2$ (Nanayakkara et al., 2012; Zhang et al., 2006) or via enhanced adsorption of water due to the increased hygroscopicity induced by sulfate (Ma et al., 2019). Although the RH was controlled at less than 1 % in our experiments, water cannot be entirely removed in the introduced gas flows. In Fig. 1, there is a positive correlation between the signal intensities of the adsorbed water and sulfite/sulfate among different experimental systems.

3.1.2 Heterogeneous reaction of SO$_2$ and NO$_2$ on TiO$_2$

As reported in previous studies, the presence of NO$_2$ can promote the heterogeneous oxidation of SO$_2$ (Ma et al., 2008, 2017; Liu et al., 2012), which was also investigated in this study under both dark and illuminated conditions. The spectra regarding the reaction of 200 ppb SO$_2$ and 200 ppb NO$_2$ on TiO$_2$ under dark conditions are shown in Fig. 1c. Sulfite, sulfate, and nitrate species were observed in this reaction system. Specifically, the bands at 1361 and 1346 cm^{-1} were assigned to aggregated sulfate; bands at 1163 and 1115 cm^{-1} were related to bridging sulfate; and bands at 1074 and 1010 cm^{-1} were ascribed to monodentate sulfite (Liu et al., 2012; Yang et al., 2017, 2018). The other bands in the 1620–1370 and 1300–1240 cm^{-1} regions were due to nitrate species, including bridging nitrate (1611, 1246 cm^{-1}), bidentate nitrate (1584, 1284 cm^{-1}), and monodentate nitrate (1503, 1453 cm^{-1}) (Goodman et al., 2001a; Ma et al., 2010). The consumption of OH groups (negative peaks at 3691 and 3630 cm^{-1}) and formation of water (3310, 3191, and 3341 cm^{-1}) on the particle surface were also observed. These results indicated that SO$_2$ can be partially oxidized to sulfate in the presence of NO$_2$ under dark conditions, which is consistent with previous studies (Ma et al., 2008; Liu et al., 2012), in spite of much lower concentration levels of SO$_2$ and NO$_2$ being used in this study.

The spectra of TiO$_2$ exposed to 200 ppb SO$_2$ and 200 ppb NO$_2$ simultaneously with UV–Vis irradiation were recorded and shown in Fig. 1d. The bands at 1629, 1584, and 1503 cm^{-1} were related to nitrate species while the bands at 1344, 1284, 1177, and 1141 cm^{-1} were associated with sulfate species. Compared to the dark experiment of SO$_2$ and NO$_2$ in Fig. 1c, more sulfate species were generated with UV–Vis irradiation, which might be due to the fact that UV–Vis irradiation significantly promotes sulfate formation by generating additional active species (Shang et al., 2010; Chen et al., 2012) as in the reaction of SO$_2$ alone.

3.1.3 Heterogeneous reaction of SO$_2$ and C$_3$H$_6$ on TiO$_2$

To investigate the heterogeneous reaction with the coexistence of inorganic and organic gases on TiO$_2$, propene was chosen as a representative volatile organic compound, and its effect on the heterogeneous oxidation of SO$_2$ was studied. Under dark conditions, the in situ spectra after introduction of 200 ppb SO$_2$ + 200 ppb C$_3$H$_6$ were recorded and are shown in Fig. 1e. No distinguishable products were observed except for the bands at 1074 and 1048 cm^{-1}, which were assigned to monodentate sulfite. Compared to the reaction of SO$_2$ alone, the coexistence of C$_3$H$_6$ had no apparent effect in this dark experiment. With UV–Vis irradiation, the sulfate bands are between 1360 and 1100 cm^{-1} with peaks at 1343, 1289, 1244, 1177, and 1139 cm^{-1} increasing with reaction time, as shown in Fig. 1f. Compared to the reaction of SO$_2$ alone with UV–Vis irradiation, similar peaks in spectra were
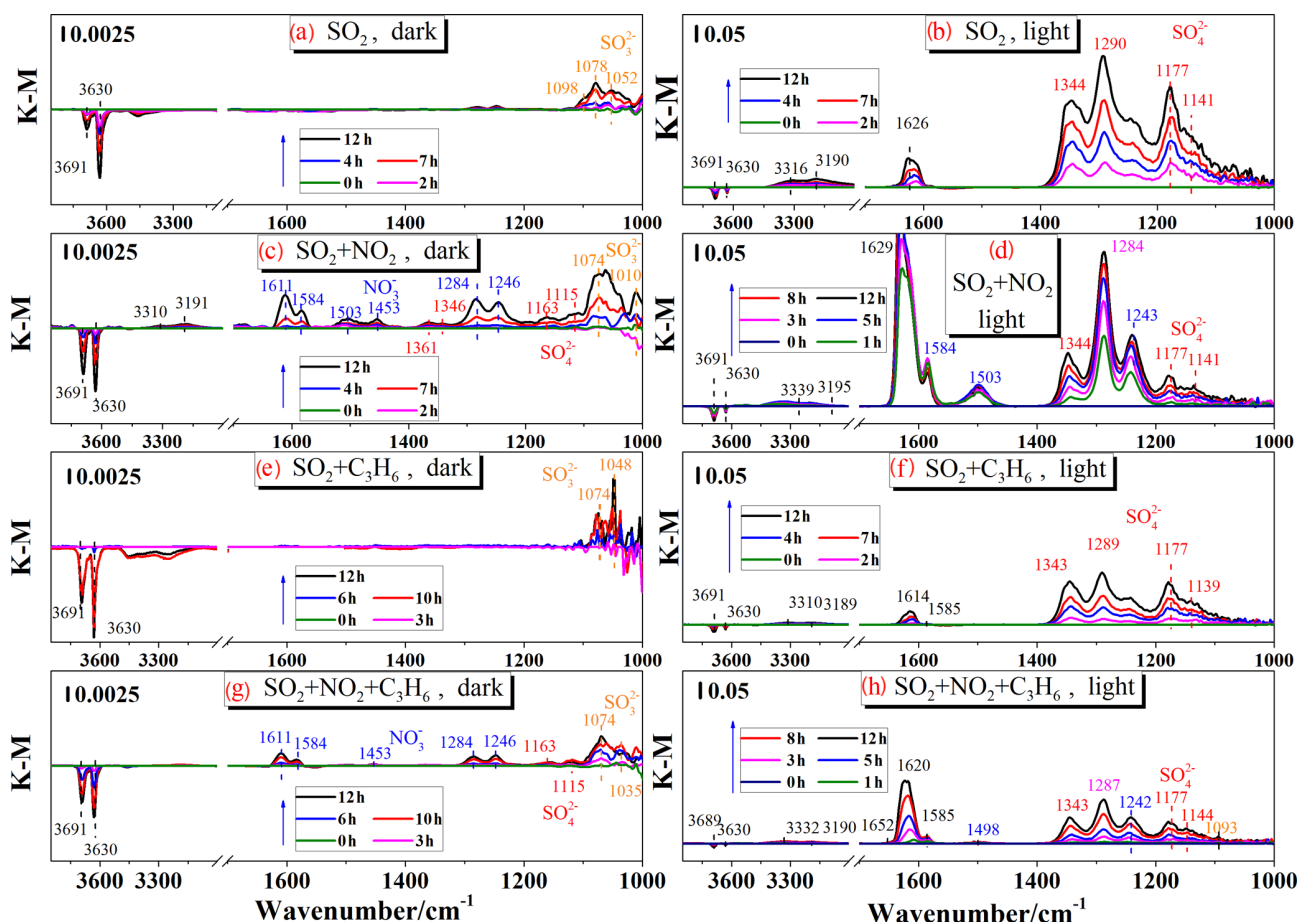
Figure 1. Dynamic changes in the in situ DRIFTS spectra of the TiO$_2$ sample as a function of time at 303 K in a flow of 20 % O$_2$ + 80 % N$_2$ with 200 ppb SO$_2$ under dark conditions **(a)** and with UV–Vis light **(b)**; with 200 ppb SO$_2$ + 200 ppb NO$_2$ under dark conditions **(c)** or with UV–Vis light **(d)**; with 200 ppb SO$_2$ + 200 ppb C$_3$H$_6$ under dark conditions **(e)** or with UV–Vis light **(f)**; with 200 ppb SO$_2$ + 200 ppb NO$_2$ + 200 ppb C$_3$H$_6$+ under dark conditions **(g)** or with UV–Vis light **(h)**.

obtained for the SO$_2$ + C$_3$H$_6$ reaction but the intensities were lower.

3.1.4 Heterogeneous reaction of SO₂, NO₂, and C₃H₆ on TiO₂

In order approximate the complexity of the real atmosphere, we investigated the heterogeneous reaction of SO$_2$, NO$_2$, and C$_3$H$_6$ on TiO$_2$. Figure 1g and h show the dynamic changes in the spectra after introducing these three gases together on TiO$_2$ under dark conditions and with UV–Vis irradiation, respectively. The concentrations of SO$_2$, NO$_2$, and C$_3$H$_6$ were all 200 ppb. The reaction of SO$_2$/NO$_2$/C$_3$H$_6$ on TiO$_2$ included both the SO$_2$/NO$_2$ reaction (Fig. 1c and d) and the SO$_2$/C$_3$H$_6$ reaction (Fig. 1e and f) under dark conditions and with UV–Vis irradiation, respectively. Thus, the products included sulfite, nitrate, and some sulfate under dark conditions, while mainly sulfate and nitrate with UV–Vis irradiation.

3.2 Sulfate formation and the influence of NO₂ and C₃H₆

To obtain the area of an individual band for quantitative analysis, a curve-fitting procedure was used employing Lorenz and Gaussian curves based on the second-derivative spectrum to deconvolute overlapping bands. An example of the analysis for the bands in Fig. 1b, with a correlation coefficient of 0.992, is shown in Fig. S2 in the Supplement. The band at 1070 cm^{-1} is attributed to sulfite, while the bands at 1140, 1178, 1240, 1292, and 1346 cm^{-1} are attributed to sulfate. To avoid interference by nitrate species and other surface products in reactions with the presence of NO$_2$, the peaks at 1198–1135 cm^{-1} were chosen for calculation of the sulfate K-M integrated area.

The K-M integrated areas of bridging sulfate in the four reaction systems: (1) SO$_2$; (2) SO$_2$ + C$_3$H$_6$; (3) SO$_2$ + NO$_2$; and (4) SO$_2$ + NO$_2$ + C$_3$H$_6$ in the dark and with UV–Vis light are shown in Fig. 2a and b, respectively. In the dark experiments, no apparent sulfate was generated in the reaction of

Table 1. Vibrational frequencies of chemisorbed species formed on TiO$_2$.

Surface species		Frequencies (cm^{-1})	References
SO$_3^{2-}$/HSO$_3^-$	monodentate sulfite	1098, 1078, 1052	Liu et al. (2012), Nanayakkara et al. (2012)
SO$_4^{2-}$	state of aggregation	1344	Nanayakkara et al. (2012)
	bidentate	1290	Yang et al. (2005)
	bridging	1177, 1141	Chen et al. (2007)
NO$_3^-$	bridging	1611, 1246	Goodman et al. (2001b), Underwood et al. (1999), Hadjiivanov and Knözinger (2000)
	bidentate	1584, 1284	Hadjiivanov and Knözinger (2000)
	monodentate	1503, 1453	Piazzesi et al. (2006)
HNO$_3$		1682	Goodman et al. (2001a)
COO$^-$		1585, 1541	Busca et al. (1987), Idriss et al. (1995), Rachmady and Vannice (2002a), Mattsson and Österlund (2010)
−CH$_3$		1452, 1379	Busca et al. (1987)
−CH		1361	Rachmady and Vannice (2002b)
−CHO		1745	Liao et al. (2001)
H$_2$O	bending vibration	1626	Goodman et al. (1999)
OH	isolated bicoordinated (on Ti atoms)	3690	Primet et al. (1971)
	H bonded	3631	Tsyganenko and Filimonov (1973) Ferretto and Glisenti (2003)
OH	adsorbed water	3456, 3310, 3190	Tarbuck and Richmond (2006)
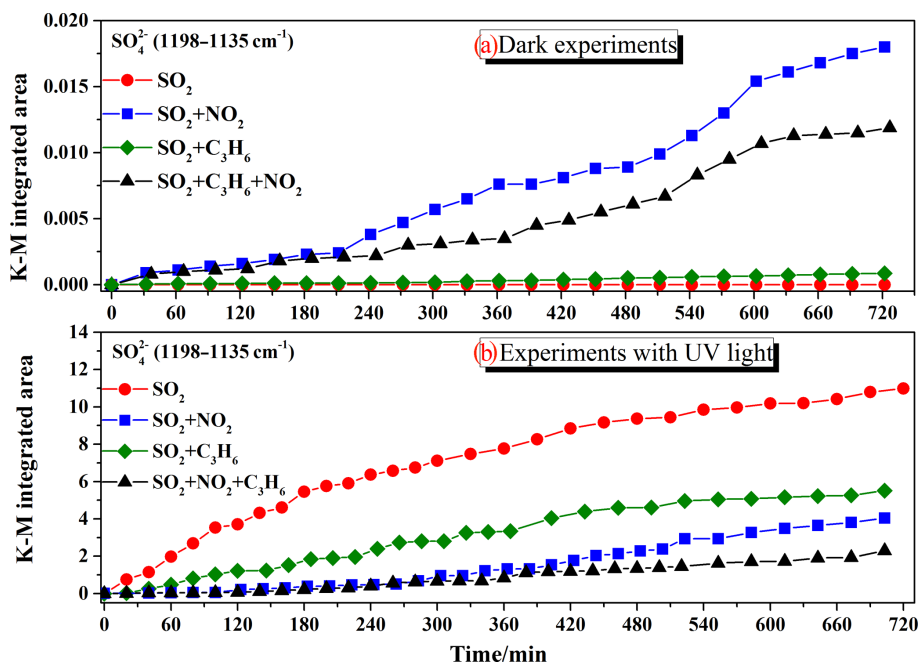
Figure 2. Integrated absorbance of the sulfate band (1198–1135 cm^{-1}) observed during the reaction of 200 ppb SO$_2$, 200 ppb SO$_2$ + 200 ppb NO$_2$, 200 ppb SO$_2$ + 200 ppb C$_3$H$_6$, 200 ppb SO$_2$ + 200 ppb NO$_2$ + 200 ppb C$_3$H$_6$ in dark experiments (**a**) and experiments with UV–Vis light (**b**).

SO$_2$ alone. The presence of C$_3$H$_6$ had no discernible effect on the formation of sulfate in dark experiments. The presence of NO$_2$ promoted the oxidation of SO$_2$ on TiO$_2$, with the result that mostly sulfate was yielded from the reaction of SO$_2$ + NO$_2$. The presence of NO$_2$ seemed to induce the generation of some ROS, which oxidize S(IV) to S(VI) on TiO$_2$ (Ma et al., 2008, 2017; Liu et al., 2012). The detailed mechanism for this effect has not been fully explored and will be discussed later. It has also been proposed that aqueous oxidation of SO$_2$ by NO$_2$ (as an oxidizing agent) contributed to significant sulfate formation in haze events (Wang et al., 2016b; Cheng et al., 2016). This reaction should not be the main pathway in the reaction systems in this study since the experiments were carried out under dry conditions (RH < 1 %), although water can still exist, as we mentioned earlier. When SO$_2$ was introduced into the cell with NO$_2$ and C$_3$H$_6$ together, sulfate formation was less than that in the reaction of SO$_2$ + NO$_2$, probably due to the competition between SO$_2$ and C$_3$H$_6$ for the ROS due to NO$_2$. In the UV–Vis irradiation experiments, on the contrary, both NO$_2$ and C$_3$H$_6$ had a distinct suppressing effect on the sulfate formation compared to the individual reaction of SO$_2$. The opposite effect of NO$_2$ on sulfate formation relative to dark experiments may be explained by the different influence of NO$_2$ on the oxidation capacity in the heterogeneous photooxidation, compared to dark experiments. In dark experiments, the contribution of NO$_2$ to the oxidation capacity is predominantly due to the limited availability of ROS, while it becomes of lesser importance when surface ROS are continuously generated in the experiments with UV–Vis irradiation. What is more, the nitrate formation from oxidation of NO$_2$ might block some surface reactive sites, and therefore resulted in less sulfate formation in the reaction of SO$_2$ + NO$_2$ than that of SO$_2$ alone with UV–Vis irradiation. To further probe and analyze the total amounts of sulfate in different systems, the samples after reaction in the different experiments were also analyzed by IC. The results, which are shown in Fig. 3, are consistent with the results derived from integrated peak areas in Fig. 2. Since formaldehyde was added to inhibit the oxidation of sulfite to sulfate in the solution, there is a possibility that HMS would be generated in the solution and be measured as sulfate (Moch et al., 2018). However, the possible interference by HMS in the measurement of sulfate by IC will not influence our conclusions on the effects of NO$_2$ and C$_3$H$_6$, since the K-M integrated area of sulfate in the In situ DRIFTS spectra were also compared. Despite the different yields of sulfate under different atmospheres, the presence of UV–Vis irradiation always increased sulfate formation significantly. We also observed that the promotion effect of UV–Vis irradiation on the heterogeneous oxidation of SO$_2$ was most significant for the individual reaction of SO$_2$, while it became less noticeable under more complex pollution, i.e., in the presence of NO$_2$ and some VOCs.
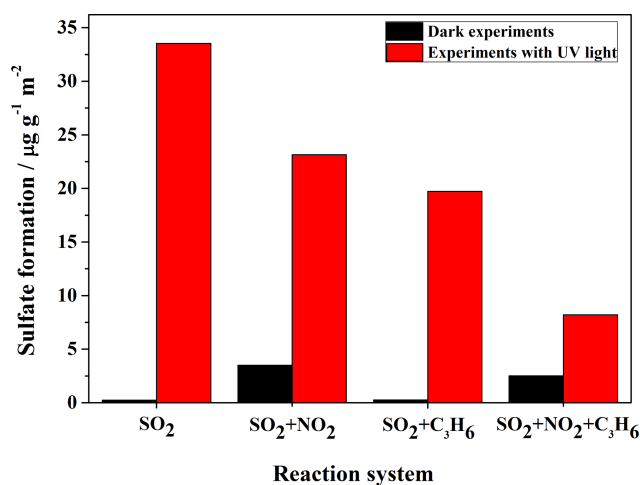

Figure 3. Ion chromatography results of the amounts of sulfate (product per unit mass divided by surface area of sample) formed on the surface of TiO$_2$ after reaction with SO$_2$, SO$_2$ + NO$_2$, SO$_2$ + C$_3$H$_6$, and SO$_2$+C$_3$H$_6$+NO$_2$ in experiments under dark conditions or with UV–Vis light. Since formaldehyde was added to inhibit the oxidation of sulfite to sulfate in the solution, there is a possibility that HMS would be generated in the solution and would be measured as sulfate.

3.3 Step-by-step experiments with UV–Vis irradiation and related mechanisms

In the step-by-step experiments, the spectra for TiO$_2$ exposure to 200 ppm NO$_2$ after the first step are shown by the black lines in Fig. 4a. The nitrate bands at 1611, 1586, 1507, 1288, and 1241 cm^{-1} increased in intensity. When the NO$_2$ was cut off, the particles were purged with air for 1 h, and the spectrum was recorded as the blue line in Fig. 4a. Air purging did not noticeably change the spectra, except that the nitrate band at 1611 cm^{-1} shifted to 1637 cm^{-1} due to the absorption of water (Ma et al., 2010), indicating a relatively steady adsorption of nitrate species. Then the NO$_2$-preadsorbed TiO$_2$ particles were exposed to SO$_2$ in the third step, marked by red lines in Fig. 4a. A new band at 1168 cm^{-1} assigned to sulfate appeared and the bands at 1350–1200 cm^{-1} became broader due to the formation of sulfate. Meanwhile, the nitrate bands at 1586 and 1507 cm^{-1} decreased in intensity and even disappeared. The possible reason might be either the replacement of nitrite by sulfate from SO$_2$ heterogeneous photooxidation (Park et al., 2017) or the photolysis of nitrate (Ye et al., 2017).

In the 200 ppm C$_3$H$_6$ presaturated experiment, which is shown in Fig. 4b, after C$_3$H$_6$ was introduced into the reaction cell for 2 h, intense bands at 1582, 1541, 1452, 1379, and 1361 cm^{-1} were observed. These principal bands are assigned to carboxylate (−COO: 1582, 1541 cm^{-1}) methyl (−CH$_3$: 1452, 1379 cm^{-1}), and methyne (−CH: 1361 cm^{-1}) (Busca et al., 1987; Idriss et al., 1995). Based on the above bands, the main products could be deemed to be formate
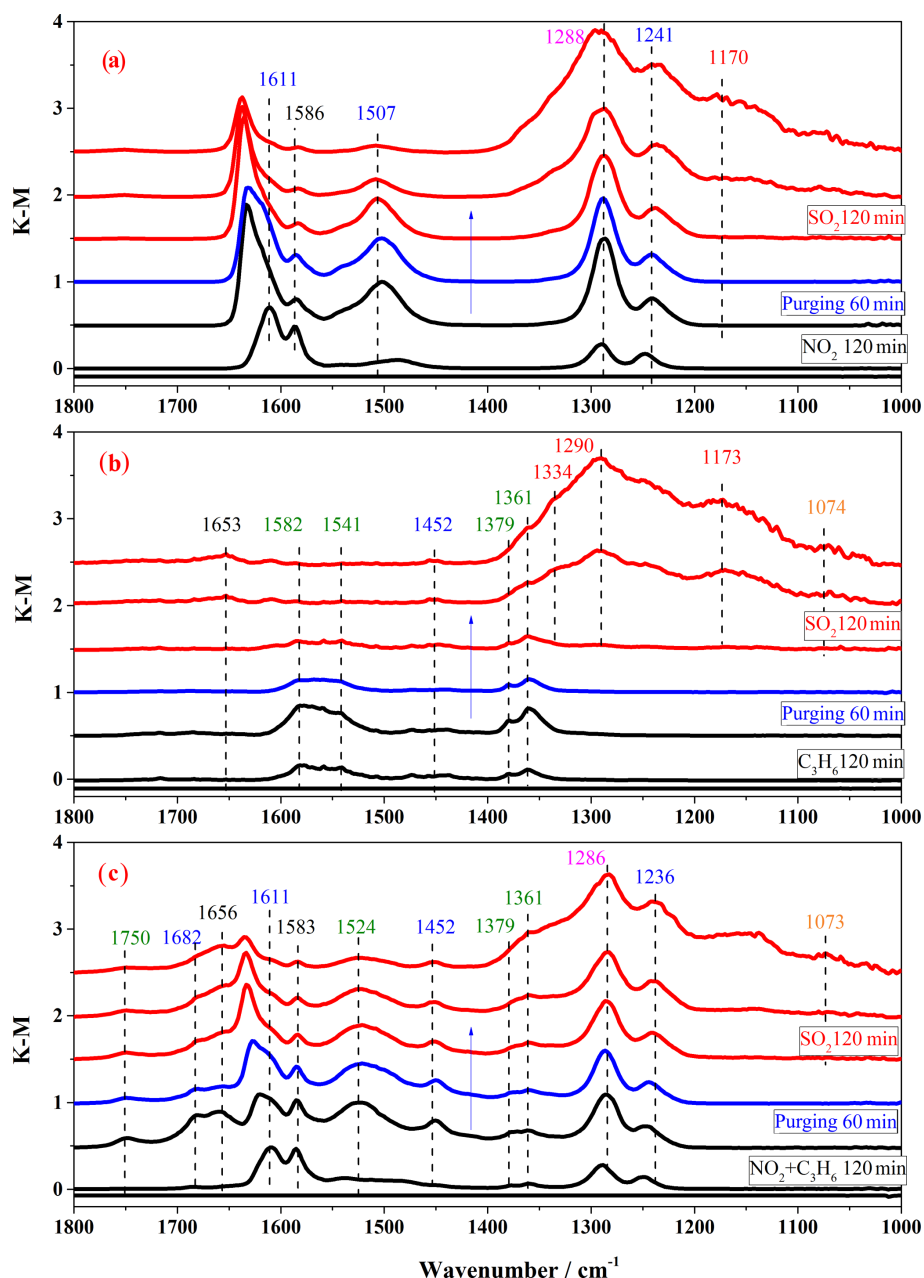
Figure 4. In situ DRIFTS spectra of surface products on TiO$_2$ in the step-by-step exposure experiments with irradiation: **(a)** exposure to 200 ppm NO$_2$ for 2 h (black lines), after purging 1 h (blue line), and then to 200 ppm SO$_2$ for 2 h (red lines); **(b)** exposure to 200 ppm C$_3$H$_6$ for 2 h (black lines), after purging 1 h (blue line), and then to 200 ppm SO$_2$ for 2 h (red lines); **(c)** exposure to 200 ppm NO$_2$ + 200 ppm C$_3$H$_6$ for 2 h (black lines), after purging 1 h (blue line), and then to 200 ppm SO$_2$ for 2 h (red lines).

and acetate species. After stopping the flow of C$_3$H$_6$ and flushing the cell with synthetic air for 1 h, the band areas of surface products were reduced, indicating that these species from C$_3$H$_6$ were not stable and could be removed easily from the surface. The subsequent introduction of SO$_2$ into the system resulted in sulfate formation, as seen by the bands in the 1380–1050 cm^{-1} region. Introducing NO$_2$ and C$_3$H$_6$ together before SO$_2$ resulted in both nitrate and organic species

on TiO$_2$, as shown in Fig. 4c. It is interesting that some distinct new bands were observed when the surface was exposed to NO$_2$ + C$_3$H$_6$, such as the bands at 1750, 1682, and 1524 cm^{-1}, which could be assigned to CH$_2$O (Liao et al., 2001), HNO$_3$ (Goodman et al., 2001a), and COO groups (Mattsson and Österlund, 2010), respectively. This may indicate some interaction between NO$_2$ and C$_3$H$_6$ and a possible
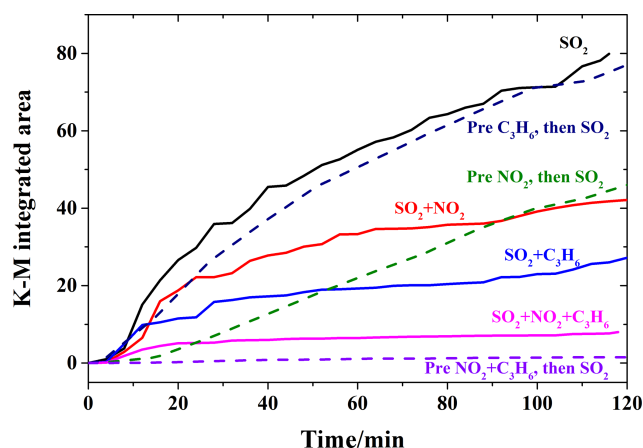
Figure 5. Integrated absorbance of the sulfate band ($1168\,cm^{-1}$) for the illuminated reactions with UV–Vis light of $200\,ppm\,SO_2$ (black, solid), $200\,ppm\,SO_2$ on a $200\,ppm\,C_3H_6$-presaturated surface (blue, dashed), $200\,ppm\,SO_2 + 200\,ppm\,NO_2$ (red, solid), $200\,ppm\,SO_2$ on a $200\,ppm\,NO_2$-presaturated surface (green, dashed), $200\,ppm\,SO_2 + 200\,ppm\,C_3H_6$ (blue, solid), $200\,ppm\,SO_2 + 200\,ppm\,NO_2 + 200\,ppm\,C_3H_6$ (pink, solid), and $200\,ppm\,SO_2$ on a $200\,ppm\,NO_2 + 200\,ppm\,C_3H_6$-presaturated surface (purple, dashed).

influence of C_3H_6 on nitrate formation, as well as NO_2 on C_3H_6 oxidation in the heterogeneous photooxidation.

Figure 5 compares the K-M integrated areas of bridging sulfate ($1168\,cm^{-1}$) formed during these step-by-step experiments under different conditions. Compared to the reaction with SO_2 alone, the pre-adsorption of C_3H_6 on TiO_2 did not have any apparent influence. This is consistent with the supposition that the formate and acetate species from heterogeneous oxidation of C_3H_6 might be easily removed from the surface. Since introducing C_3H_6 with SO_2 together suppressed sulfate formation in the heterogeneous photooxidation, while pre-adsorption of C_3H_6 had little influence, C_3H_6 is proposed to compete with SO_2 for ROS rather than surface reactive sites in the heterogeneous photooxidation. Instead, the pre-adsorption of NO_2 on TiO_2 suppressed the formation of sulfate, which might have resulted from the different absorption status of the oxidation products of NO_2 and C_3H_6. Compared to the experiment introducing NO_2 and SO_2 simultaneously, sulfate formation was more inhibited with pre-adsorption of NO_2 in the first hour, while sulfate formation in these two cases became similar after 1.5 h duration. This may indicate that NO_2 suppressed sulfate formation, mainly due to the competition between SO_2 and NO_2 for surface reactive sites. Compared to the individual reaction of SO_2, both pre-adsorption of NO_2 and introducing NO_2 simultaneously suppressed sulfate formation from the beginning of the heterogeneous photooxidation. It is interesting that pre-adsorption with $NO_2 + C_3H_6$ resulted in much less sulfate formation compared to the pre-adsorption of NO_2 or C_3H_6, as well as the reaction of $SO_2 + NO_2 + C_3H_6$. Although

the detailed reason for this phenomenon was not discovered in this study, a possible reason might be that the oxidation products from NO_2 and C_3H_6 blocked some reactive sites on TiO_2 and suppressed sulfate formation in heterogeneous photooxidation, since NO_2 and C_3H_6 were cut off after pre-adsorption and ROS were expected to be generated on TiO_2 with UV–Vis irradiation. According to the DRIFTS spectra in Fig. 4c, besides nitrate, aldehydes ($1750\,cm^{-1}$) and carboxylic acids ($1524\,cm^{-1}$) were also observed on TiO_2 after pre-adsorption with $NO_2 + C_3H_6$.
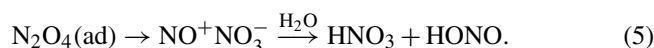
4 Discussion

4.1 Dark reactions

The heterogeneous oxidation of SO_2 on TiO_2 has been investigated by many previous studies. The following mechanisms for SO_2 adsorption on TiO_2 surfaces have been proposed in previous studies (Nanayakkara et al., 2012):
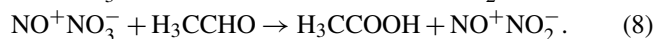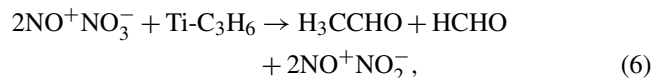
$$\text{Ti-OH} + SO_2 \rightarrow \text{Ti-OSO}_2\text{H}, \qquad (1)$$

$$2\text{Ti-OH} + SO_2 \rightarrow Ti_2 - SO_3 \cdot H_2O, \qquad (2)$$

$$\text{Ti-O}^{2-} + SO_2 \rightarrow \text{Ti-SO}_3^{2-}. \qquad (3)$$
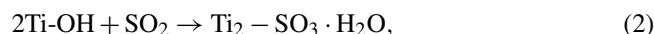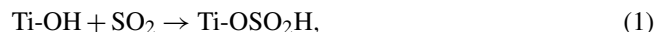
These adsorption processes result in the conversion of SO_2 to sulfite (S(IV)) on the surface. It has been demonstrated that coexisting NO_2 can induce the generation of some ROS, which oxidize S(IV) to S(VI) on mineral oxides (Ma et al., 2008, 2017; Liu et al., 2012). There were several possible responsible ROS proposed in previous studies, although the detailed mechanism has not yet been fully explored. One possible ROS is N_2O_4, which can undergo hydrolysis to N(III) and N(V) species (Liu et al., 2012; Finlayson-Pitts et al., 2003; Li et al., 2018). These reactive nitrogen species can oxidize S(IV) to S(VI) (Wang et al., 2016b; Li et al., 2018).

$$2\text{Ti-NO}_2 \rightarrow Ti_2 - N_2O_4, \qquad (4)$$

$$N_2O_4(\text{ad}) \rightarrow NO^+NO_3^- \xrightarrow{H_2O} HNO_3 + HONO. \qquad (5)$$

Besides N_2O_4, NO_2 may also react directly with surface OH and form HNO_3 on TiO_2 (C. Liu et al., 2017). The HNO_3 generated through this pathway may also contribute to the oxidation of S(IV) to S(VI). It has also been proposed that aqueous oxidation of SO_2 by NO_2 (as an oxidizing agent) contributed to significant sulfate formation in haze events (Wang et al., 2016b; Cheng et al., 2016). This aqueous reaction should not be significant in the reaction systems of this study due to the limited amount of water under low RH conditions ($< 1\,\%$ RH).

When C_3H_6 was introduced together with NO_2, sulfate formation was less than that in the reaction of $SO_2 + NO_2$, probably due to the reaction between C_3H_6 and the reactive nitrogen species. The detailed mechanism was not explored
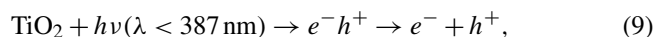
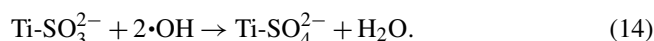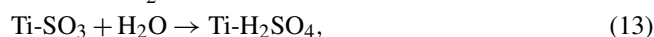in this study. The following reactions may take place in this process.

$$2NO^+NO_3^- + Ti\text{-}C_3H_6 \rightarrow H_3CCHO + HCHO$$
$$+ 2NO^+NO_2^-, \quad (6)$$

$$NO^+NO_3^- + HCHO \rightarrow HCOOH + NO^+NO_2^-, \quad (7)$$

$$NO^+NO_3^- + H_3CCHO \rightarrow H_3CCOOH + NO^+NO_2^-. \quad (8)$$

Heterogeneous reactions between NO$_2$ and organics can also lead to nitro-organics on hexane soot (Kwamena and Abbatt, 2008; Al-Abadleh and Grassian, 2000), which may also occur on the surface of TiO$_2$, and these products blocked some reactive sites for sulfate formation.
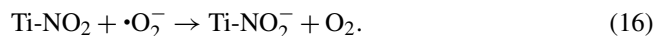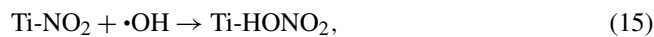
4.2 Light reactions

With UV illumination, TiO$_2$ can be excited by UV light ($\lambda < 387$ nm), then the photogenerated electrons and holes can react with H$_2$O and O$_2$ to produce additional ROS (primarily $\cdot$O$_2^-$ and $\cdot$OH), and oxidize more SO$_2$ to sulfate on TiO$_2$ than that produced under dark conditions (Shang et al., 2010; Chen et al., 2012). The detailed mechanism was summarized by Chen et al. (2012) and references therein:

$$TiO_2 + h\nu(\lambda < 387\,nm) \rightarrow e^-h^+ \rightarrow e^- + h^+, \quad (9)$$

$$O_2 + e^- \rightarrow \cdot O_2^-, \quad (10)$$

$$H_2O + h^+ \rightarrow \cdot OH + H^+. \quad (11)$$

Then the SO$_2$ can react with these ROS and promote the formation of sulfate (Shang et al., 2010):

$$Ti\text{-}SO_2 + \cdot O_2^- \rightarrow Ti\text{-}SO_3 + O^-, \quad (12)$$

$$Ti\text{-}SO_3 + H_2O \rightarrow Ti\text{-}H_2SO_4, \quad (13)$$

$$Ti\text{-}SO_3^{2-} + 2\cdot OH \rightarrow Ti\text{-}SO_4^{2-} + H_2O. \quad (14)$$

In the UV–Vis irradiation experiments, NO$_2$ had a distinct suppressing effect on the sulfate formation compared to the individual reaction of SO$_2$. Rather than resulting in ROS formation and oxidation of S(IV) to S(VI) in dark experiments, the main reaction of NO$_2$ with the surface ROS resulted in nitrate and nitrite formation in experiments with UV–Vis irradiation (Ndour et al., 2008; Yu and Jang, 2018).

$$Ti\text{-}NO_2 + \cdot OH \rightarrow Ti\text{-}HONO_2, \quad (15)$$

$$Ti\text{-}NO_2 + \cdot O_2^- \rightarrow Ti\text{-}NO_2^- + O_2. \quad (16)$$

The nitrate or nitrite generated from the oxidation of NO$_2$ might block some surface reactive sites, since in the step-to-step experiments the pre-adsorption of NO$_2$ on TiO$_2$ also suppressed the formation of sulfate and resulted in similar sulfate formation to that in the experiment introducing NO$_2$ and SO$_2$ simultaneously. The competition between SO$_2$ and NO$_2$ for surface reactive sites might be the main reason for the fact that the coexistence of NO$_2$ with SO$_2$ resulted in decreased sulfate formation with UV–Vis irradiation in this study. Although Gen et al. (2019) found that photolysis of nitrate enhanced sulfate formation in wet aerosols, this mechanism may not be applied in this study since the reaction system is quite different from their study. The ROS, which oxidize S(IV) to S(VI), are mainly $\cdot$O$_2^-$ and $\cdot$OH in the presence of UV–Vis irradiation rather than the photolysis of nitrate.

C$_3$H$_6$ also had a distinct suppressing effect on sulfate formation. Similar to NO$_2$, C$_3$H$_6$ will react with surface ROS.

$$C_3H_6 \xrightarrow{\cdot OH} RCHO \xrightarrow{\cdot OH} RCOOH \xrightarrow{\cdot OH} CO_2 + H_2O, \quad (17)$$

where R represents H or an alkyl group. These gaseous products in the photooxidation of C$_3$H$_6$ do not seem to block surface reactive sites, which can explain why the pre-adsorption of C$_3$H$_6$ on TiO$_2$ did not show an obvious suppressing effect on the formation of sulfate in the step-by-step experiment.

When C$_3$H$_6$ and NO$_2$ were introduced simultaneously into the reaction system together with SO$_2$, both competed for ROS with SO$_2$ and therefore resulted in the lowest formation of sulfate among the heterogeneous reactions. Besides, in the step-by-step experiments, the pre-adsorption of C$_3$H$_6$ and NO$_2$ on TiO$_2$ suppressed sulfate formation significantly, which indicated that lots of reactive sites for SO$_2$ oxidation might be blocked by these oxidation products in pre-adsorption with UV–Vis irradiation. Karagulian et al. (2009) found that nitrite can induce the photooxidation of VOCs on airborne particles and produce organic nitrates and carbonyl compounds. Thus, the formation of organic nitrates may be an important factor to suppress the formation of sulfate due to the blocking effect.

5 Conclusions and environmental implications

Based on the experimental results obtained in this study, we propose the following possible mechanisms for the reaction of SO$_2$ in the presence of NO$_2$ and C$_3$H$_6$ under conditions close to those in the real atmosphere. Under dark conditions at 303 K, SO$_2$ could hardly react on the particle surface and only a few sulfite-like species formed. With reaction time increasing, the adsorption sites on the surface became saturated with sulfite and prevented SO$_2$ from adsorbing on the particles further. Coexisting NO$_2$ could enhance the heterogeneous formation of sulfate with much lower concentrations (200 ppb) relative to previous studies ($\sim$ 100 ppm) (Ma et al., 2008; Liu et al., 2012; Zhao et al., 2018). The presence of C$_3$H$_6$ had little effect on sulfate formation in the heterogeneous reaction of SO$_2$ but suppressed sulfate formation in the heterogeneous reaction of SO$_2$ and NO$_2$, because C$_3$H$_6$ could react ROS generated in the adsorption of NO$_2$. When irradiation was introduced into the system, the ROS such as $\cdot$OH and $\cdot$O$_2^-$ could initiate photocatalytic oxidation of S(IV) species to sulfate. Sulfate formation was suppressed significantly with the coexistence of NO$_2$ and/or C$_3$H$_6$ in the presence of UV–Vis light. The formation of nitrate, car-

bonyl compounds, and organic nitrate consumed both available ROS and surface reactive sites.

These results indicated that heterogeneous oxidation of SO$_2$ might be influenced by the coexisting inorganic and organic gas pollutants under complex pollution conditions due to the competition for ROS and active surface sites among them. In this study, only one VOC was investigated, but the heterogeneous oxidation of various VOCs has been reported in previous studies (Niu et al., 2017; Du et al., 2000). When a VOC and SO$_2$ coexist, the competition for ROS and surface reactive sites between the VOC and SO$_2$ is likely to suppress sulfate formation in the heterogeneous reactions, such as that observed for the presence of CH$_3$CHO on α-Fe$_2$O$_3$ in dark experiments (Zhao et al., 2015), the presence of C$_7$H$_{16}$ on TiO$_2$ with UV–Vis irradiation (Du et al., 2000), and the presence of C$_3$H$_6$ on TiO$_2$ under dark condition or with UV–Vis irradiation in this study. Due to the different properties of the oxidation products, the influence of coexisting VOCs might be different for different VOC species and on different mineral dusts. Some coexisting VOCs, such as HCOOH on α-Fe$_2$O$_3$ (Wu et al., 2013), and HCHO in aerosol water (Moch et al., 2018; Song et al., 2019) might enhance sulfate formation. These results highlighted the very complex heterogeneous reaction processes that take place under complex air pollution conditions due to the ubiquitous interactions between organic and inorganic species. For better estimation of heterogeneous sulfate formation, the kinetics of the heterogeneous oxidation of SO$_2$ must be developed with consideration of the influence of coexisting VOCs and other inorganic gases.

Author contributions. QM, BC, and HH designed the study. YW, WY, and BC carried out the experiments. BC, WY, JM, and QM analyzed the data with input from all co-authors. BC and YW wrote the paper with contribution from YL, JM, WY, and PZ on the editing of the paper.

References

Al-Abadleh, H. A. and Grassian, V. H.: Heterogeneous reaction of NO$_2$ on hexane soot: A Knudsen cell and FT-IR study, J. Phys. Chem. A, 104, 11926–11933, https://doi.org/10.1021/Jp002918i, 2000.

Armaroli, T., Becue, T., and Gautier, S.: Diffuse reflection infrared spectroscopy (DRIFTS): Application to the in situ analysis of catalysts, Oil & Gas Science and Technology-Revue D Ifp Energies Nouvelles, 59, 215–237, https://doi.org/10.2516/Ogst:2004016, 2004.

Busca, G., Lamotte, J., Lavalley, J. C., and Lorenzelli, V.: FT-IR study of the adsorption and transformation of formaldehyde on oxide surfaces, J. Am. Chem. Soc., 109, 5197–5202, 1987.

Capaldo, K., Corbett, J. J., Kasibhatla, P., Fischbeck, P., and Pandis, S. N.: Effects of ship emissions on sulphur cycling and radiative climate forcing over the ocean, Nature, 400, 743–746, 1999.

Chen, H., Kong, L., Chen, J., Zhang, R., and Wang, L.: Heterogeneous uptake of carbonyl sulfide on hematite and hematite-NaCl mixtures, Environ. Sci. Technol., 41, 6484–6490, 2007.

Chen, H. H., Nanayakkara, C. E., and Grassian, V. H.: Titanium Dioxide Photocatalysis in Atmospheric Chemistry, Chem. Rev., 112, 5919–5948, https://doi.org/10.1021/Cr3002092, 2012.

Cheng, Y., Zheng, G., Wei, C., Mu, Q., Zheng, B., Wang, Z., Gao, M., Zhang, Q., He, K., Carmichael, G., Poschl, U., and Su, H.: Reactive nitrogen chemistry in aerosol water as a source of sulfate during haze events in China, Sci. Adv., 2, e1601530, https://doi.org/10.1126/sciadv.1601530, 2016.

Chu, B., Zhang, X., Liu, Y., He, H., Sun, Y., Jiang, J., Li, J., and Hao, J.: Synergetic formation of secondary inorganic and organic aerosol: effect of SO$_2$ and NH$_3$ on particle formation and growth, Atmos. Chem. Phys., 16, 14219–14230, https://doi.org/10.5194/acp-16-14219-2016, 2016.

Cwiertny, D. M., Young, M. A., and Grassian, V. H.: Chemistry and photochemistry of mineral dust aerosol, Annu. Rev. Phys. Chem., 59, 27–51, https://doi.org/10.1146/annurev.physchem.59.032607.093630, 2008.

Davidson, C. I., Phalen, R. F., and Solomon, P. A.: Airborne particulate matter and human health: a review, Aerosol Sci. Technol., 39, 737–749, https://doi.org/10.1080/02786820500191348, 2005.

Dentener, F. J., Carmichael, G. R., Zhang, Y., Lelieveld, J., and Crutzen, P. J.: Role of mineral aerosol as a reactive surface in the global troposphere, J. Geophys. Res.-Atmos., 101, 22869–22889, 1996.

Du, Y.-G., Shang, J., and Xu, Z.-l.: Photocatalytic Reaction of Sulfur Dioxide With Heptane in the Gas-Phase Over Titanium Dioxide, Chem. Res., 16, 203–207, 2000.

Ferretto, L. and Glisenti, A.: Surface acidity and basicity of a rutile powder, Chem. Mater., 15, 1181–1188, 2003.

Finlayson-Pitts, B. J., Wingen, L. M., Sumner, A. L., Syomin, D., and Ramazan, K. A.: The heterogeneous hydrolysis of NO$_2$ in laboratory systems and in outdoor and indoor atmospheres: An integrated mechanism, Phys. Chem. Chem. Phys., 5, 223–242, https://doi.org/10.1039/b208564j, 2003.

Fu, H., Wang, X., Wu, H., Yin, Y., and Chen, J.: Heterogeneous uptake and oxidation of SO2 on iron oxides, J. Phys. Chem. C, 111, 6077–6085, 2007.

Gen, M., Zhang, R., Huang, D. D., Li, Y., and Chan, C. K.: Heterogeneous Oxidation of SO2 in Sulfate Production during Nitrate Photolysis at 300 nm: Effect of pH, Relative Humidity, Irradiation Intensity, and the Presence of Organic Compounds, Environ. Sci. Technol., 53, 8757–8766, https://doi.org/10.1021/acs.est.9b01623, 2019.

George, C., Ammann, M., D'Anna, B., Donaldson, D. J., and Nizkorodov, S. A.: Heterogeneous Photochemistry in the Atmosphere, Chem. Rev., 115, 4218–4258, 2015.

Goodman, A., Underwood, G., and Grassian, V.: Heterogeneous reaction of NO$_2$: Characterization of gas-phase and adsorbed products from the reaction, 2NO$_2$(g) + H$_2$O(a) → HONO(g) + HNO$_3$(a) on hydrated silica particles, J. Phys. Chem. A, 103, 7217–7223, 1999.

Goodman, A. L., Bernard, E. T., and Grassian, V. H.: Spectroscopic Study of Nitric Acid and Water Adsorption on Oxide Particles: Enhanced Nitric Acid Uptake Kinetics in the Presence of Adsorbed Water, J. Phys. Chem. A, 105, 6443–6457, https://doi.org/10.1021/jp003722l, 2001a.

Goodman, A. L., Li, P., Usher, C., and Grassian, V.: Heterogeneous uptake of sulfur dioxide on aluminum and magnesium oxide particles, J. Phys. Chem. A, 105, 6109–6120, 2001b.

Hadjiivanov, K. and Knözinger, H.: Species formed after NO adsorption and NO + O$_2$ co-adsorption on TiO$_2$: an FTIR spectroscopic study, Phys. Chem. Chem. Phys., 2, 2803–2806, 2000.

He, H., Wang, Y., Ma, Q., Ma, J., Chu, B., Ji, D., Tang, G., Liu, C., Zhang, H., and Hao, J.: Mineral dust and NO$_x$ promote the conversion of SO$_2$ to sulfate in heavy pollution days, Sci. Rep.-UK, 4, 04172, https://doi.org/10.1038/srep04172, 2014.

Hug, S. J.: In Situ Fourier Transform Infrared Measurements of Sulfate Adsorption on Hematite in Aqueous Solutions, J. Colloid Interf. Sci., 188, 415–422, 1997.

Idriss, H., Diagne, C., Hindermann, J., Kiennemann, A., and Barteau, M.: Reactions of acetaldehyde on CeO$_2$ and CeO$_2$-supported catalysts, J. Catal., 155, 219–237, 1995.

Jang, M. S. and Kamens, R. M.: Characterization of secondary aerosol from the photooxidation of toluene in the presence of NO$_x$ and 1-propene, Environ. Sci. Technol., 35, 3626–3639, https://doi.org/10.1021/es010676+, 2001.

Jaoui, M., Edney, E. O., Kleindienst, T. E., Lewandowski, M., Offenberg, J. H., Surratt, J. D., and Seinfeld, J. H.: Formation of secondary organic aerosol from irradiated α-pinene/toluene/NO$_x$ mixtures and the effect of isoprene and sulfur dioxide, J. Geophys. Res., 113, D09303, https://doi.org/10.1029/2007jd009426, 2008.

Jayne, J., Davidovits, P., Worsnop, D., Zahniser, M., and Kolb, C.: Uptake of sulfur dioxide (G) by aqueous surfaces as a function of pH: the effect of chemical reaction at the interface, J. Phys. Chem., 94, 6041–6048, 1990.

Karagulian, F., Dilbeck, C. W., and Finlayson-Pitts, B. J.: Nitrite-Induced Oxidation of Organic Coatings on Models for Airborne Particles, J. Phys. Chem. A, 113, 7205–7212, https://doi.org/10.1021/jp808419g, 2009.

Kwamena, N. O. A. and Abbatt, J. P. D.: Heterogeneous nitration reactions of polycyclic aromatic hydrocarbons and n-hexane soot by exposure to NO$_3$/NO$_2$/N$_2$O$_5$, Atmos. Environ., 42, 8309–8314, https://doi.org/10.1016/j.atmosenv.2008.07.037, 2008.

Li, L., Chen, Z. M., Zhang, Y. H., Zhu, T., Li, J. L., and Ding, J.: Kinetics and mechanism of heterogeneous oxidation of sulfur dioxide by ozone on surface of calcium carbonate, Atmos. Chem. Phys., 6, 2453–2464, https://doi.org/10.5194/acp-6-2453-2006, 2006.

Li, L., Hoffmann, M. R., and Colussi, A. J.: Role of Nitrogen Dioxide in the Production of Sulfate during Chinese Haze-Aerosol Episodes, Environ. Sci. Technol., 52, 2686–2693, https://doi.org/10.1021/acs.est.7b05222, 2018.

Liao, L. F., Lien, C. F., and Lin, J. L.: FTIR study of adsorption and photoreactions of acetic acid on TiO$_2$, Phys. Chem. Chem. Phys., 3, 3831–3837, https://doi.org/10.1039/B103419g, 2001.

Liu, C., Ma, Q. X., Liu, Y. C., Ma, J. Z., and He, H.: Synergistic reaction between SO$_2$ and NO$_2$ on mineral oxides: a potential formation pathway of sulfate aerosol, Phys. Chem. Chem. Phys., 14, 1668–1676, https://doi.org/10.1039/c1cp22217a, 2012.

Liu, C., Ma, Q. X., He, H., He, G. Z., Ma, J. Z., Liu, Y. C., and Wu, Y.: Structure-activity relationship of surface hydroxyl groups during NO$_2$ adsorption and transformation on TiO$_2$ nanoparticles, Environ. Sci.-Nano, 4, 2388–2394, https://doi.org/10.1039/c7en00920h, 2017.

Liu, X. G., Li, J., Qu, Y., Han, T., Hou, L., Gu, J., Chen, C., Yang, Y., Liu, X., Yang, T., Zhang, Y., Tian, H., and Hu, M.: Formation and evolution mechanism of regional haze: a case study in the megacity Beijing, China, Atmos. Chem. Phys., 13, 4501–4514, https://doi.org/10.5194/acp-13-4501-2013, 2013.

Liu, Z. R., Xie, Y. Z., Hu, B., Wen, T. X., Xin, J. Y., Li, X. R., and Wang, Y. S.: Size-resolved aerosol water-soluble ions during the summer and winter seasons in Beijing: Formation mechanisms of secondary inorganic aerosols, Chemosphere, 183, 119–131, https://doi.org/10.1016/j.chemosphere.2017.05.095, 2017.

Ma, J., Chu, B., Liu, J., Liu, Y., Zhang, H., and He, H.: NO$_x$ promotion of SO$_2$ conversion to sulfate: An important mechanism for the occurrence of heavy haze during winter in Beijing, Environ. Pollut., 233, 662–669, https://doi.org/10.1016/j.envpol.2017.10.103, 2018.

Ma, Q., Liu, Y., and He, H.: Synergistic Effect between NO$_2$ and SO$_2$ in Their Adsorption and Reaction on γ-Alumina, J. Phys. Chem. A, 112, 6630–6635, 2008.

Ma, Q., He, H., and Liu, Y.: In situ DRIFTS study of hygroscopic behavior of mineral aerosol, J. Environ. Sci., 22, 555–560, 2010.

Ma, Q., Wang, T., Liu, C., He, H., Wang, Z., Wang, W., and Liang, Y.: SO$_2$ Initiates the Efficient Conversion of NO$_2$ to HONO on MgO Surface, Environ. Sci. Technol., 51, 3767–3775, https://doi.org/10.1021/acs.est.6b05724, 2017.

Ma, Q. X., Wang, L., Chu, B. W., Ma, J. Z., and He, H.: Contrary Role of H$_2$O and O$_2$ in the Kinetics of Heterogeneous Photochemical Reactions of SO$_2$ on TiO$_2$, J. Phys. Chem. A, 123, 1311–1318, https://doi.org/10.1021/acs.jpca.8b11433, 2019.

Mattsson, A. and Österlund, L.: Adsorption and Photoinduced Decomposition of Acetone and Acetic Acid on Anatase, Brookite, and Rutile TiO$_2$ Nanoparticles, J. Phys. Chem. C, 114, 14121–14132, https://doi.org/10.1021/jp103263n, 2010.

Moch, J. M., Dovrou, E., Mickley, L. J., Keutsch, F. N., Cheng, Y., Jacob, D. J., Jiang, J. K., Li, M., Munger, J. W., Qiao, X. H., and Zhang, Q.: Contribution of Hydroxymethane Sulfonate to Ambient Particulate Matter: A Potential Explanation for High Particulate Sulfur During Severe Winter Haze in Beijing, Geophys. Res. Lett., 45, 11969–11979, https://doi.org/10.1029/2018GL079309, 2018.

Nanayakkara, C. E., Pettibone, J., and Grassian, V. H.: Sulfur dioxide adsorption and photooxidation on isotopically-labeled titanium dioxide nanoparticle surfaces: roles of surface hydroxyl groups and adsorbed water in the formation and stability of adsorbed sulfite and sulfate, Phys. Chem. Chem. Phys., 14, 6957–6966, https://doi.org/10.1039/c2cp23684b, 2012.

Ndour, M., D'Anna, B., George, C., Ka, O., Balkanski, Y., Kleffmann, J., Stemmler, K., and Ammann, M.: Photoenhanced uptake of NO$_2$ on mineral dust: Laboratory experiments and model simulations, Geophys. Res. Lett., 35, L05812, https://doi.org/10.1029/2007gl032006, 2008.

Niu, H. J. Y., Li, K. Z., Chu, B. W., Su, W. K., and Li, J. H.: Heterogeneous Reactions between Toluene and NO$_2$ on Mineral Particles under Simulated Atmospheric Conditions, Environ. Sci. Technol., 51, 9596–9604, https://doi.org/10.1021/acs.est.7b00194, 2017.

Odum, J. R., Hoffmann, T., Bowman, F., Collins, D., Flagan, R. C., and Seinfeld, J. H.: Gas/particle partitioning and secondary organic aerosol yields, Environ. Sci. Technol., 30, 2580–2585, 1996.

Park, J., Jang, M., and Yu, Z.: Heterogeneous Photo-oxidation of SO$_2$ in the Presence of Two Different Mineral Dust Particles: Gobi and Arizona Dust, Environ. Sci. Technol., 51, 9605–9613, https://doi.org/10.1021/acs.est.7b00588, 2017.

Peak, D., Ford, R. G., and Sparks, D. L.: An in situ ATR-FTIR investigation of sulfate bonding mechanisms on goethite, J. Colloid Interf. Sci., 218, 289–299, 1999.

Piazzesi, G., Elsener, M., Kröcher, O., and Wokaun, A.: Influence of NO$_2$ on the hydrolysis of isocyanic acid over TiO$_2$, Appl. Catal. B-Environ., 65, 169–174, 2006.

Pöschl, U.: Atmospheric aerosols: composition, transformation, climate and health effects, Angew. Chem. Int. Ed., 44, 7520–7540, https://doi.org/10.1002/anie.200501122, 2005.

Primet, M., Pichat, P., and Mathieu, M. V.: Infrared study of the surface of titanium dioxides. I. Hydroxyl groups, J. Phys. Chem., 75, 1216–1220, 1971.

Rachmady, W. and Vannice, M. A.: Acetic Acid Reduction to Acetaldehyde over Iron Catalysts: II. Characterization by Mössbauer Spectroscopy, DRIFTS, TPD, and TPR, J. Catal., 208, 170–179, 2002a.

Rachmady, W. and Vannice, M. A.: Acetic Acid Reduction to Acetaldehyde over Iron Catalysts: I. Kinetic Behavior, J. Catal., 208, 158–169, 2002b.

Shang, J., Li, J., and Zhu, T.: Heterogeneous reaction of SO$_2$ on TiO$_2$ particles, Science China Chemistry, 53, 2637–2643, https://doi.org/10.1007/s11426-010-4160-3, 2010.

Shen, X., Zhao, Y., Chen, Z., and Huang, D.: Heterogeneous reactions of volatile organic compounds in the atmosphere, Atmos. Environ., 68, 297–314, https://doi.org/10.1016/j.atmosenv.2012.11.027, 2013.

Song, C., Na, K., Warren, B., Malloy, Q., and Cocker, D. R.: Impact of propene on secondary organic aerosol formation from m-xylene, Environ. Sci. Technol., 41, 6990–6995, https://doi.org/10.1021/es062279a, 2007.

Song, S., Gao, M., Xu, W., Sun, Y., Worsnop, D. R., Jayne, J. T., Zhang, Y., Zhu, L., Li, M., Zhou, Z., Cheng, C., Lv, Y., Wang, Y., Peng, W., Xu, X., Lin, N., Wang, Y., Wang, S., Munger, J. W., Jacob, D. J., and McElroy, M. B.: Possible heterogeneous chemistry of hydroxymethanesulfonate (HMS) in northern China winter haze, Atmos. Chem. Phys., 19, 1357–1371, https://doi.org/10.5194/acp-19-1357-2019, 2019.

Tang, M., Larish, W. A., Fang, Y., Gankanda, A., and Grassian, V. H.: Heterogeneous Reactions of Acetic Acid with Oxide Surfaces: Effects of Mineralogy and Relative Humidity, J. Phys. Chem. A, 120, 5609–5616, https://doi.org/10.1021/acs.jpca.6b05395, 2016.

Tarbuck, T. L. and Richmond, G. L.: Adsorption and Reaction of CO$_2$ and SO$_2$ at a Water Surface, J. Am. Chem. Soc., 128, 3256–3267, 2006.

Thalman, R., de Sá, S. S., Palm, B. B., Barbosa, H. M. J., Pöhlker, M. L., Alexander, M. L., Brito, J., Carbone, S., Castillo, P., Day, D. A., Kuang, C., Manzi, A., Ng, N. L., Sedlacek III, A. J., Souza, R., Springston, S., Watson, T., Pöhlker, C., Pöschl, U., Andreae, M. O., Artaxo, P., Jimenez, J. L., Martin, S. T., and Wang, J.: CCN activity and organic hygroscopicity of aerosols downwind of an urban region in central Amazonia: seasonal and diel variations and impact of anthropogenic emissions, Atmos. Chem. Phys., 17, 11779–11801, https://doi.org/10.5194/acp-17-11779-2017, 2017.

Tsyganenko, A. and Filimonov, V.: Infrared spectra of surface hydroxyl groups and crystalline structure of oxides, J. Mol. Struct., 19, 579–589, 1973.

Underwood, G., Miller, T., and Grassian, V.: Transmission FT-IR and Knudsen cell study of the heterogeneous reactivity of gaseous nitrogen dioxide on mineral oxide particles, J. Phys. Chem. A, 103, 6184–6190, 1999.

Usher, C. R., Al-Hosney, H., Carlos-Cuellar, S., and Grassian, V. H.: A laboratory study of the heterogeneous uptake and oxidation of sulfur dioxide on mineral dust particles, J. Geophys. Res.-Atmos., 107, 4713, https://doi.org/10.1029/2002jd002051, 2002.

Wang, G., Cheng, S. Y., Wei, W., Zhou, Y., Yao, S., and Zhang, H. Y.: Characteristics and source apportionment of VOCs in the suburban area of Beijing, China, Atmos. Pollut. Res., 7, 711–724, https://doi.org/10.1016/j.apr.2016.03.006, 2016a.

Wang, G. H., Zhang, R. Y., Gomez, M. E., Yang, L. X., Zamora, M. L., Hu, M., Lin, Y., Peng, J. F., Guo, S., Meng, J. J., Li, J. J., Cheng, C. L., Hu, T. F., Ren, Y. Q., Wang, Y. S., Gao, J., Cao, J. J., An, Z. S., Zhou, W. J., Li, G. H., Wang, J. Y., Tian, P. F., Marrero-Ortiz, W., Secrest, J., Du, Z. F., Zheng, J., Shang, D. J.,

Zeng, L. M., Shao, M., Wang, W. G., Huang, Y., Wang, Y., Zhu, Y. J., Li, Y. X., Hu, J. X., Pan, B., Cai, L., Cheng, Y. T., Ji, Y. M., Zhang, F., Rosenfeld, D., Liss, P. S., Duce, R. A., Kolb, C. E., and Molina, M. J.: Persistent sulfate formation from London Fog to Chinese haze, P. Natl. Acad. Sci. USA, 113, 13630–13635, https://doi.org/10.1073/pnas.1616540113, 2016b.

Wang, T., Liu, Y., Deng, Y., Fu, H., Zhang, L., and Chen, J. M.: Emerging investigator series: Heterogeneous reaction of sulfur dioxide on mineral dust nanoparticles: from single component to mixed components, Environ. Sci.: Nano, 5, 1821–1833, https://doi.org/10.1039/C8EN00376A, 2018.

Wang, Y., Yao, L., Wang, L., Liu, Z., Ji, D., Tang, G., Zhang, J., Sun, Y., Hu, B., and Xin, J.: Mechanism for the formation of the January 2013 heavy haze pollution episode over central and eastern China, Science China Earth Sciences, 57, 14–25, https://doi.org/10.1007/s11430-013-4773-4, 2014a.

Wang, Y., Zhang, Q., Jiang, J., Zhou, W., Wang, B., He, K., Duan, F., Zhang, Q., Philip, S., and Xie, Y.: Enhanced sulfate formation during China's severe winter haze episode in January 2013 missing from current models, J. Geophys. Res.-Atmos., 119, 10425–10440, https://doi.org/10.1002/2013jd021426, 2014b.

Wu, L. Y., Tong, S. R., Zhou, L., Wang, W. G., and Ge, M. F.: Synergistic effects between SO$_2$ and HCOOH on alpha-Fe$_2$O$_3$, J. Phys. Chem. A, 117, 3972–3979, https://doi.org/10.1021/jp400195f, 2013.

Yang, F., Tan, J., Zhao, Q., Du, Z., He, K., Ma, Y., Duan, F., Chen, G., and Zhao, Q.: Characteristics of PM$_{2.5}$ speciation in representative megacities and across China, Atmos. Chem. Phys., 11, 5207–5219, https://doi.org/10.5194/acp-11-5207-2011, 2011.

Yang, Q., Xie, C., Xu, Z., Gao, Z., and Du, Y.: Synthesis of highly active sulfate-promoted rutile titania nanoparticles with a response to visible light, J. Phys. Chem. B, 109, 5554–5560, 2005.

Yang, S., Yuesi, W., and Changchun, Z.: Measurement of the vertical profile of atmospheric SO$_2$ during the heating period in Beijing on days of high air pollution, Atmos. Environ., 43, 468–472, https://doi.org/10.1016/j.atmosenv.2008.09.057, 2009.

Yang, W., He, H., Ma, Q., Ma, J., Liu, Y., Liu, P., and Mu, Y.: Synergistic formation of sulfate and ammonium resulting from reaction between SO$_2$ and NH$_3$ on typical mineral dust, Phys. Chem. Chem. Phys., 18, 956–964, https://doi.org/10.1039/c5cp06144j, 2016.

Yang, W., Ma, Q., Liu, Y., Ma, J., Chu, B., Wang, L., and He, H.: Role of NH$_3$ in the Heterogeneous Formation of Secondary Inorganic Aerosols on Mineral Oxides, J. Phys. Chem. A, 122, 6311–6320, https://doi.org/10.1021/acs.jpca.8b05130, 2018.

Yang, W., Ma, Q., Liu, Y., Ma, J., Chu, B., and He, H.: The effect of water on the heterogeneous reactions of SO$_2$ and NH$_3$ on the surfaces of α-Fe$_2$O$_3$ and γ-Al$_2$O$_3$, Environ. Sci.: Nano, 6, 2749–2758, https://doi.org/10.1039/C9EN00574A, 2019.

Yang, W. W., Zhang, J. H., Ma, Q. X., Zhao, Y., Liu, Y. C., and He, H.: Heterogeneous Reaction of SO2 on Manganese Oxides: the Effect of Crystal Structure and Relative Humidity, Sci. Rep.-UK, 7, 4550, https://doi.org/10.1038/S41598-017-04551-6, 2017.

Ye, C., Zhang, N., Gao, H., and Zhou, X.: Photolysis of Particulate Nitrate as a Source of HONO and NO$_x$, Environ. Sci. Technol., 51, 6849–6856, https://doi.org/10.1021/acs.est.7b00387, 2017.

Yu, T., Zhao, D., Song, X., and Zhu, T.: NO$_2$-initiated multiphase oxidation of SO$_2$ by O$_2$ on CaCO$_3$ particles, Atmos. Chem. Phys., 18, 6679–6689, https://doi.org/10.5194/acp-18-6679-2018, 2018.

Yu, Z. and Jang, M.: Simulation of heterogeneous photooxidation of SO$_2$ and NO$_x$ in the presence of Gobi Desert dust particles under ambient sunlight, Atmos. Chem. Phys., 18, 14609–14622, https://doi.org/10.5194/acp-18-14609-2018, 2018.

Zhang, T., Cao, J. J., Tie, X. X., Shen, Z. X., Liu, S. X., Ding, H., Han, Y. M., Wang, G. H., Ho, K. F., Qiang, J., and Li, W. T.: Water-soluble ions in atmospheric aerosols measured in Xi'an, China: Seasonal variations and sources, Atmos. Res., 102, 110–119, https://doi.org/10.1016/j.atmosres.2011.06.014, 2011.

Zhang, X. Y., Zhuang, G. S., Chen, J. M., Wang, Y., Wang, X., An, Z. S., and Zhang, P.: Heterogeneous reactions of sulfur dioxide on typical mineral particles, J. Phys. Chem. B, 110, 12588–12596, https://doi.org/10.1021/jp0617773, 2006.

Zhang, Y., Tong, S. R., Ge, M. F., Jing, B., Hou, S. Q., Tan, F., Chen, Y., Guo, Y. C., and Wu, L. Y.: The formation and growth of calcium sulfate crystals through oxidation of SO$_2$ by O$_3$ on size-resolved calcium carbonate, Rsc Advances, 8, 16285–16293, https://doi.org/10.1039/c8ra02050g, 2018.

Zhao, D., Song, X., Zhu, T., Zhang, Z., Liu, Y., and Shang, J.: Multiphase oxidation of SO$_2$ by NO$_2$ on CaCO$_3$ particles, Atmos. Chem. Phys., 18, 2481–2493, https://doi.org/10.5194/acp-18-2481-2018, 2018.

Zhao, X., Kong, L., Sun, Z., Ding, X., Cheng, T., Yang, X., and Chen, J.: Interactions between Heterogeneous Uptake and Adsorption of Sulfur Dioxide and Acetaldehyde on Hematite, J. Phys. Chem. A, 119, 4001–4008, https://doi.org/10.1021/acs.jpca.5b01359, 2015.

Zheng, B., Zhang, Q., Zhang, Y., He, K. B., Wang, K., Zheng, G. J., Duan, F. K., Ma, Y. L., and Kimoto, T.: Heterogeneous chemistry: a mechanism missing in current models to explain secondary inorganic aerosol formation during the January 2013 haze episode in North China, Atmos. Chem. Phys., 15, 2031–2049, https://doi.org/10.5194/acp-15-2031-2015, 2015.

Zou, Y., Deng, X. J., Zhu, D., Gong, D. C., Wang, H., Li, F., Tan, H. B., Deng, T., Mai, B. R., Liu, X. T., and Wang, B. G.: Characteristics of 1 year of observational data of VOCs, NO$_x$ and O$_3$ at a suburban site in Guangzhou, China, Atmos. Chem. Phys., 15, 6625–6636, https://doi.org/10.5194/acp-15-6625-2015, 2015.